CHAPTER

THIRTEEN

THEORY OF PHOTOELASTICITY

13.1 INTRODUCTION

In Chap. 11, the working optical instrument of photoelasticity, a polariscope, was described in detail. The purpose of this chapter is to discuss the theory of photoelasticity, i.e., what happens in the polariscope when a photoelastic model is placed in the field and loaded. This discussion will be kept as simple as possible, yet it will be sufficiently complete to describe most of the photoelastic effects that can be observed in a transmission polariscope.

13.2 TEMPORARY DOUBLE REFRACTION [1–3]

Many transparent noncrystalline materials that are optically isotropic when free of stress become optically anisotropic and display characteristics similar to crystals when they are stressed. These characteristics persist while loads on the material are maintained but disappear when the loads are removed. This behavior, known as *temporary double refraction*, was first observed by Sir David Brewster in 1816. The method of photoelasticity is based on this physical behavior of transparent noncrystalline materials.

In Chap. 1 it was shown that at least three mutually perpendicular planes, which are free of shear stress, exist at each point of a loaded body. These planes were defined as principal planes and the normal stresses acting on them were defined as the principal stresses σ_1, σ_2, and σ_3. In general, the three principal

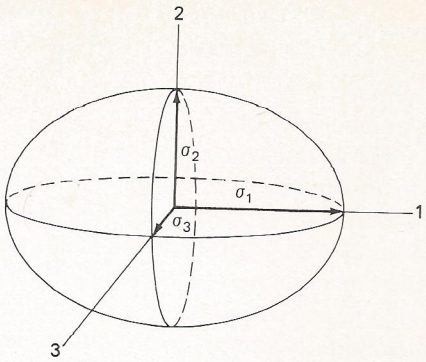

Figure 13.1 The stress ellipsoid.

stresses at a point have different magnitudes. The resultant stress T_n on any plane through the point can be expressed in terms of the three principal stresses at the point and the direction cosines associated with the plane by means of Eqs. (1.15). Normal and shear stresses on the plane for a particular set of coordinate directions can be obtained from Eqs. (1.16).

A geometric representation that provides considerable physical insight into the nature of the state of stress at a point is known as the *stress ellipsoid* or the *ellipsoid of Lamé*. An equation for this stress ellipsoid, shown in Fig. 13.1, is obtained by solving Eqs. (1.15) for the direction cosines and adding the sum of the squares to obtain

$$\frac{T_{nx}^2}{\sigma_1^2} + \frac{T_{ny}^2}{\sigma_2^2} + \frac{T_{nz}^2}{\sigma_3^2} = 1 \tag{13.1}$$

Each radius of this ellipsoid represents the magnitude of the resultant stress T_n on some plane through the point. Since Eqs. (1.15) were expressed in terms of the principal directions, the semiaxes of the ellipsoid represent the magnitudes of the principal stresses at the point. The particular plane associated with an arbitrary radius must be determined by some auxiliary construction such as the stress-director surface [2, p. 65].

The intersection of an arbitrary plane through the origin with the surface of the stress ellipsoid is an ellipse. On planes through the point which have normals along one of the semiaxes of the ellipse, the resultant stress can be resolved into a normal component and a shear component in a direction perpendicular to the plane of the ellipse. The shear stress component in a direction parallel to the plane of the ellipse is zero. The normal stress component on such a plane is known as a *secondary principal stress*. Later it will be shown that the optical response of a doubly refracting material for light passage at normal incidence to the plane of the ellipse is not affected by the presence of this shear stress component or by the normal stress component in a direction perpendicular to the plane of the ellipse. Secondary principal stresses play an important role in three-dimensional photoelasticity studies.

The optical anisotropy (temporary double refraction) which develops in a material as a result of stress can also be represented by an ellipsoid, known in this

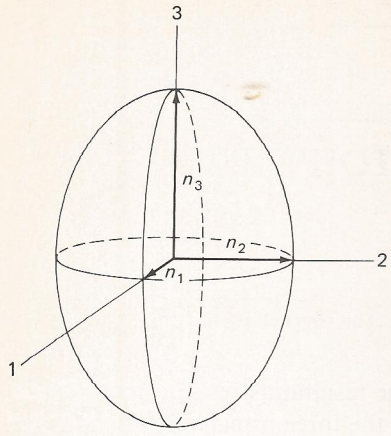

Figure 13.2 The index ellipsoid.

case as the *index ellipsoid*. The semiaxes of the index ellipsoid represent the principal indices of refraction of the material at the point, as shown in Fig. 13.2. Any radius of the ellipsoid represents a direction of light propagation through the point. A plane through the origin, which is perpendicular to the radius, intersects the ellipsoid as an ellipse. The semiaxes of the ellipse represent the indices of refraction associated with light waves having planes of vibration which contain the radius vector and an axis of the ellipse. For a material which is optically isotropic, the three principal indices of refraction are equal, and the index ellipsoid becomes a sphere. The index of refraction is then the same for all directions of light propagation through the material.

The similarities which exist between the stress-ellipsoid representation of the state of stress at a point in a loaded body and the index-ellipsoid representation of the optical properties of a material exhibiting temporary double refraction suggest the presence of a relationship between the two quantities which may form the basis for an experimental determination of stresses (or strains). The relationship is known as the *stress-optic law*.

13.3 THE STRESS-OPTIC LAW [3–7]

The theory which relates changes in the indices of refraction of a material exhibiting temporary double refraction to the state of stress in the material is due to Maxwell, who reported the phenomenon in 1853. Maxwell noted that the changes in the indices of refraction were linearly proportional to the loads (thus to the stresses or strains for a linearly elastic material) and followed the relationships

$$\begin{aligned} n_1 - n_0 &= c_1\sigma_1 + c_2(\sigma_2 + \sigma_3) \\ n_2 - n_0 &= c_1\sigma_2 + c_2(\sigma_3 + \sigma_1) \\ n_3 - n_0 &= c_1\sigma_3 + c_2(\sigma_1 + \sigma_2) \end{aligned} \tag{13.2}$$

where $\sigma_1, \sigma_2, \sigma_3$ = principal stresses at point
n_0 = index of refraction of material in unstressed state
n_1, n_2, n_3 = indices of refraction of material in stressed state associated with principal stress directions (principal indices of refraction)
c_1, c_2 = constants known as stress-optic coefficients

Equations (13.2) are the fundamental relationships between stress and optical effect and are known as the stress-optic law. These equations indicate that the complete state of stress at a point can be determined by measuring the three principal indices of refraction and establishing the directions of the three principal optical axes. Since the measurements are extremely difficult to make in the three-dimensional case, practical application has been limited to cases of plane stress ($\sigma_3 = 0$). For plane-stress situations, Eqs. (13.2) reduce to

$$n_1 - n_0 = c_1\sigma_1 + c_2\sigma_2 \qquad n_2 - n_0 = c_1\sigma_2 + c_2\sigma_1 \tag{13.3}$$

Favre [6] has used a Mach-Zender interferometer and Post [7] has used a series interferometer to make measurements of absolute retardations. Such measurements permitted direct determination of the individual principal stresses at interior points of a loaded two-dimensional model. Measurements with an interferometer can be very precise, but they are difficult and time-consuming. For this reason, absolute-retardation methods are seldom used, while the method of photoelasticity, which utilizes relative retardations, enjoys wide application.

13.4 THE STRESS-OPTIC LAW IN TERMS OF RELATIVE RETARDATION [3, 8–15]

Equations (13.2) provide the changes in index of refraction experienced by a material exhibiting temporary double refraction as the result of an applied state of stress. In the previous section, it was indicated that these absolute changes in index of refraction can be used as the basis for a stress-measurement method. The more widely used method of photoelasticity, however, makes use of relative rather than absolute changes in index of refraction. For example, consider the equations obtained by eliminating n_0 from Eqs. (13.2):

$$\begin{aligned} n_2 - n_1 &= (c_2 - c_1)(\sigma_1 - \sigma_2) = c(\sigma_1 - \sigma_2) \\ n_3 - n_2 &= (c_2 - c_1)(\sigma_2 - \sigma_3) = c(\sigma_2 - \sigma_3) \\ n_1 - n_3 &= (c_2 - c_1)(\sigma_3 - \sigma_1) = c(\sigma_3 - \sigma_1) \end{aligned} \tag{13.4}$$

where $c = c_2 - c_1$ is the relative stress-optic coefficient expressed in terms of brewsters (1 brewster $= 10^{-13}$ cm^2/dyn $= 10^{-12}$ m^2/N $= 6.895 \times 10^{-9}$ in^2/lb). Materials exhibiting temporary double refraction may display the properties of either positive or negative crystals. In a positive crystal like quartz, the extraordinary index of refraction n_e is greater than the ordinary index n_o. In a negative crystal like calcite the opposite is true. Photoelastic materials are considered to

exhibit positive birefringence when the velocity of propagation of the light wave associated with the principal stress σ_1 is greater than the velocity of the wave associated with the principal stress σ_2. Since the principal stresses are ordered such that $\sigma_1 \geq \sigma_2 \geq \sigma_3$, the principal indices of refraction of a positive doubly refracting material can be ordered such that $n_3 \geq n_2 \geq n_1$. The form of Eqs. (13.4) has been selected to make the relative stress-optic coefficient c a positive constant.

Since a stressed photoelastic model behaves like a temporary wave plate, Eq. (11.37) can be used to relate the relative angular phase shift Δ (or relative retardation) to changes in the indices of refraction in the material resulting from the stresses. For example, consider a slice of material (thickness h) oriented perpendicular to one of the principal-stress directions at the point of interest in the model. If a beam of plane-polarized light is passed through the slice at normal incidence, the relative retardation Δ accumulated along each of the principal-stress directions can be obtained by substituting Eq. (11.37) in turn into each of Eqs. (13.4). Thus

$$\Delta_{12} = \frac{2\pi hc}{\lambda}(\sigma_1 - \sigma_2) \qquad \Delta_{23} = \frac{2\pi hc}{\lambda}(\sigma_2 - \sigma_3) \qquad \Delta_{31} = \frac{2\pi hc}{\lambda}(\sigma_3 - \sigma_1) \tag{13.5}$$

where Δ_{12} is the magnitude of the relative angular phase shift (relative retardation) developed between components of a light beam propagating in the σ_3 direction. The two components of the beam would have electric vectors oriented in the σ_1 and σ_2 directions. The component associated with the principal stress σ_1 would propagate at a higher velocity than the one associated with the stress σ_2 (since $\sigma_1 \geq \sigma_2$) if the material exhibits positive birefringence. Similar meanings can be attached to the retardations Δ_{23} and Δ_{31}.

Equations (13.5) express the stress-optic law as it is commonly applied in photoelasticity. The relative retardation Δ is linearly proportional to the difference between the two principal stresses having directions perpendicular to the path of propagation of the light beam. The third principal stress, having a direction parallel to the path of propagation of the light beam, has no effect on the relative retardation. Also, the relative retardation Δ is linearly proportional to the model or slice thickness h and inversely proportional to the wavelength λ of the light being used.

The relative stress-optic coefficient c is usually assumed to be a material constant that is independent of the wavelength of the light being used. A study by Vandaele-Dossche and van Geen [13] has shown, however, that this coefficient may depend on wavelength in some cases as the model material passes from the elastic to the plastic state. The dependence of the relative stress-optic coefficient c on the wavelength of the light being used is referred to as *photoelastic dispersion* or *dispersion of birefringence.*

From an analysis of the general three-dimensional state of stress at a point, as represented by the stress ellipsoid, and from an analysis of the change in index of refraction with direction of light propagation in the stressed material, as repre-

sented by the index ellipsoid, it can be shown that Eqs. (13.5) apply not only for principal stresses but also for secondary principal stresses. Thus

$$\Delta' = \frac{2\pi hc}{\lambda}(\sigma'_1 - \sigma'_2) \tag{13.6}$$

where σ'_1 and σ'_2 are secondary principal stresses ($\sigma'_1 \geq \sigma'_2$) at the point of interest in directions perpendicular to the path of propagation of the light beam. The stress-optic law in terms of secondary principal stresses is widely used in three-dimensional photoelasticity work.

For two-dimensional or plane-stress problems, where one of the principal stresses is zero (say $\sigma_3 = 0$), the stress-optic law in terms of the nonzero principal stresses and for light at normal incidence to the plane of the model can be written without the subscripts on the retardation simply as

$$\Delta = \frac{2\pi hc}{\lambda}(\sigma_1 - \sigma_2) \tag{13.7}$$

Here it is understood that σ_1 and σ_2 are the in-plane principal stresses and that σ_1 is greater than σ_2 but not greater than $\sigma_3 = 0$ if both in-plane stresses are compressive.

Since brewsters are not commonly employed in engineering practice, Eq. (13.7) is frequently expressed in the following form for practical work:

$$\sigma_1 - \sigma_2 = \frac{Nf_\sigma}{h} \qquad \text{lb/in}^2 \text{ or N/m}^2 \tag{13.8}$$

where

$$N = \frac{\Delta}{2\pi} \qquad \text{dimensionless} \tag{13.9}$$

is the relative retardation in terms of a complete cycle of retardation,

$$f_\sigma = \frac{\lambda}{c} \qquad \text{lb/in or N/m} \tag{13.10}\dagger$$

is a property of the model material for a given wavelength of light known as the *material fringe value*, and h is the model thickness in inches or meters.

It is immediately apparent from Eq. (13.8) that the stress difference $\sigma_1 - \sigma_2$ in a two-dimensional model can be determined if the relative retardation N can be measured and if the material fringe value f_σ can be established by means of calibration. Actually, the function of the polariscope is to determine the value of N at each point in the model.

If a photoelastic model exhibits a perfectly linear elastic behavior, the difference in the principal strains $\epsilon_1 - \epsilon_2$ can also be measured by establishing the

† Often Eq. (13.8) is written as $\tau = (\sigma_1 - \sigma_2)/2 = Nf_\sigma/h$, where f_σ is the material fringe value in terms of shear and is equal to one-half the f_σ value defined here.

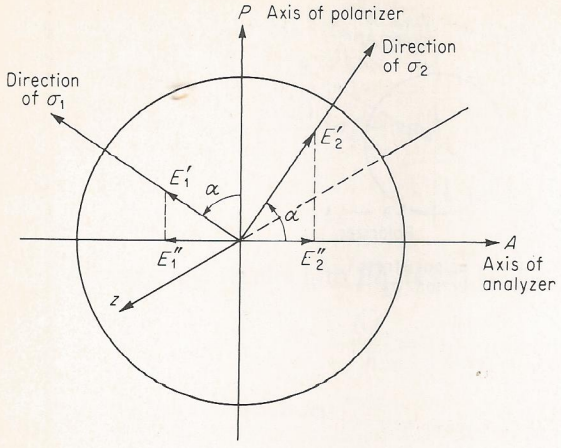

Figure 13.5 Components of the light vectors which are transmitted through the analyzer of a plane polariscope.

Thus, the waves upon emerging from the model can be expressed as

$$E_1' = k \cos \alpha \cos (\omega t - \Delta_1) \qquad E_2' = k \sin \alpha \cos (\omega t - \Delta_2) \tag{c}$$

where

$$\Delta_1 = \frac{2\pi h}{\lambda}(n_1 - 1) \qquad \Delta_2 = \frac{2\pi h}{\lambda}(n_2 - 1)$$

After leaving the model, the two components continue to propagate without further change and enter the analyzer in the manner shown in Fig. 13.5. The light components E_1' and E_2' are resolved when they enter the analyzer into horizontal components E_1'' and E_2'' and into vertical components. Since the vertical components are internally absorbed in the analyzer, they have not been shown in Fig. 13.5.

The horizontal components transmitted by the analyzer combine to produce an emerging light vector E_{ax}, which is given by

$$E_{ax} = E_2'' - E_1'' = E_2' \cos \alpha - E_1' \sin \alpha \tag{d}$$

Substituting Eqs. (c) into (d) yields

$$\begin{aligned} E_{ax} &= k \sin \alpha \cos \alpha [\cos (\omega t - \Delta_2) - \cos (\omega t - \Delta_1)] \\ &= k \sin 2\alpha \sin \frac{\Delta_2 - \Delta_1}{2} \sin \left(\omega t - \frac{\Delta_2 + \Delta_1}{2} \right) \end{aligned} \tag{13.14}$$

It is interesting to note in Eq. (13.14) that the average angular phase shift $(\Delta_2 + \Delta_1)/2$ affects the phase of the light wave emerging from the analyzer but not the amplitude (coefficient of the time-dependent term). Thus, it has no influence on the intensity (intensity is proportional to the square of the amplitude) of the light emerging from the analyzer but serves only to change the phase of the emerging wave with respect to the phase of the initial wave. The relative retardation $\Delta = \Delta_2 - \Delta_1$, however, appears in the amplitude of the wave; therefore, it is one of the factors which controls the intensity of light emerging from the analyzer.

Since the average angular phase shift $(\Delta_2 + \Delta_1)/2$ has no effect on the intensity, it does not contribute to the optical patterns observed in a photoelastic model. In future photoelasticity developments only relative retardations will be considered in order to simplify the analysis.

Since the intensity of light is proportional to the square of the amplitude of the light wave, the light emerging from the analyzer of a plane polariscope is given by

$$I = K \sin^2 2\alpha \sin^2 \frac{\Delta}{2} \tag{13.15}$$

where $$\Delta = \Delta_2 - \Delta_1 = \frac{2\pi h}{\lambda}(n_2 - n_1) = \frac{2\pi hc}{\lambda}(\sigma_1 - \sigma_2)$$

Examination of Eq. (13.15) indicates that extinction ($I = 0$) occurs either when $\sin^2 2\alpha = 0$ or when $\sin^2 (\Delta/2) = 0$. Thus, one of the conditions for extinction is related to the principal-stress directions and the other is related to the principal-stress difference.

A. Effect of Principal-Stress Directions

When $2\alpha = n\pi$, where $n = 0, 1, 2, \ldots$, $\sin^2 2\alpha = 0$ and extinction occurs. In other words, when one of the principal-stress directions coincides with the axis of the polarizer ($\alpha = 0, \pi/2$, or any exact multiple of $\pi/2$), the intensity of the light is zero. Since the analysis of the optical effects produced by a stressed model in a plane polariscope was conducted for an arbitrary point in the model, the analysis is valid for all points of the model. When the entire model is viewed in the polariscope, a fringe pattern is observed; the fringes are loci of points where the principal-stress directions (either σ_1 or σ_2) coincide with the axis of the polarizer. The fringe pattern produced by the $\sin^2 2\alpha$ term in Eq. (13.15) is known as an *isoclinic fringe pattern.* Isoclinic fringe patterns are used to determine the principal-stress directions at all points of a photoelastic model. Since isoclinics represent a very important segment of the data obtained from a photoelastic model, the topic of isoclinic-fringe-pattern interpretation will be treated in more detail in Sec. 14.3.

B. Effect of Principal-Stress Difference

When $\Delta/2 = n\pi$, where $n = 0, 1, 2, 3, \ldots$, $\sin^2 (\Delta/2) = 0$ and extinction occurs. In other words, when the principal-stress difference is either zero ($n = 0$) or sufficient to produce an integral number of wavelengths of retardation ($n = 1, 2, 3, \ldots$), the intensity of light emerging from the analyzer is zero. When a complete model is viewed in the polariscope, this second condition for extinction yields a second fringe pattern where the fringes are loci of points exhibiting the same order of extinction ($n = 0, 1, 2, 3, \ldots$). The fringe pattern produced by the $\sin^2 (\Delta/2)$ term in Eq. (13.15) is known as an *isochromatic fringe pattern.* The nature of the optical

effect producing the isochromatic fringe pattern requires some additional discussion.

Recall from Eq. (13.7) that the relative retardation Δ may be expressed as

$$\Delta = \frac{2\pi hc}{\lambda}(\sigma_1 - \sigma_2)$$

Thus

$$n = \frac{\Delta}{2\pi} = \frac{hc}{\lambda}(\sigma_1 - \sigma_2) \qquad (e)$$

Examination of Eq. (*e*) indicates that the order of extinction n depends on both the principal-stress difference $\sigma_1 - \sigma_2$ and the wavelength λ of the light being used. Thus, for a given principal-stress difference, the order of extinction n can be an integer only for light of a single wavelength (monochromatic light). When a model is viewed in monochromatic light, the isochromatic fringe pattern appears as a series of dark bands since the intensity of light is zero when $n = 0, 1, 2, 3, \ldots$. When a model is viewed with white light (all wavelengths of the visible spectrum present), the isochromatic fringe pattern appears as a series of colored bands. The intensity of light is zero, and a black fringe appears only when the principal-stress difference is zero and a zero order of extinction occurs for all wavelengths of light. No other region of zero intensity is possible since the principal-stress difference required to produce a given order of extinction is different for each of the wavelengths. Thus, not all the wavelengths can be extinguished simultaneously to produce a condition of zero intensity. The various colored bands form in regions where the principal-stress difference is sufficient to produce extinction of a particular wavelength of the white light. For example, when the principal-stress difference is sufficient to produce extinction of the green wavelengths, the complementary color, red, appears as the isochromatic fringe. At the higher levels of principal-stress difference, where several wavelengths of light can be extinguished simultaneously, e.g., second order red and third order violet, the isochromatic fringes become pale and very difficult to identify; therefore, they are seldom used for stress analysis work.

With monochromatic light, the individual fringes in an isochromatic-fringe pattern remain sharp and clear to very high orders of extinction. Since the wavelength of the light is fixed, Eq. (*e*) can be written in terms of the material fringe value f_σ and the isochromatic fringe order N as

$$n = N = \frac{h}{f_\sigma}(\sigma_1 - \sigma_2) \qquad (f)$$

Hence, the number of fringes appearing in an isochromatic fringe pattern is controlled by the magnitude of the principal-stress difference $\sigma_1 - \sigma_2$, by the thickness h of the model, and by the sensitivity of the photoelastic material, as denoted by the material fringe value f_σ.

In general, the principal-stress difference $\sigma_1 - \sigma_2$ and the principal-stress dir-

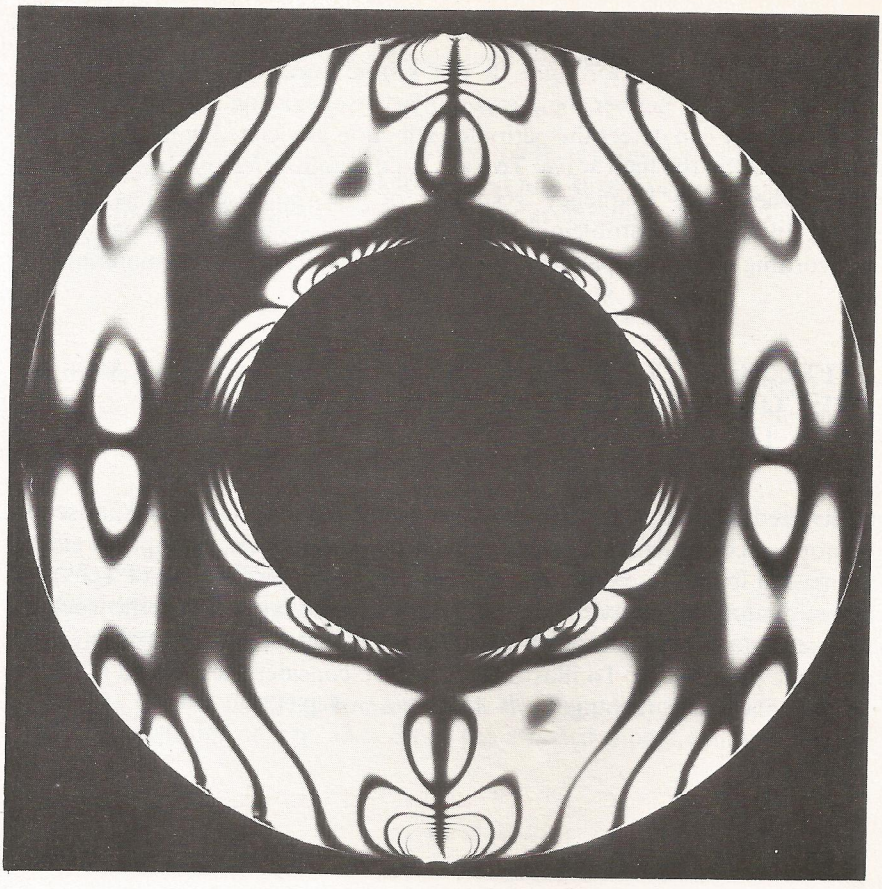

Figure 13.6 Superimposed isochromatic and isoclinic fringe patterns for a ring loaded in diametral compression.

ections vary from point to point in a photoelastic model. As a result, the isoclinic fringe pattern and the isochromatic fringe pattern are superimposed, as shown in Fig. 13.6, when the model is viewed in a plane polariscope. Separation of the patterns requires special techniques which will be discussed later.

Theoretically, the isoclinic and isochromatic fringes should be lines of zero width; however, the photograph in Fig. 13.6 shows the fringes as bands with considerable width. Also, direct visual examination of the fringe pattern in a polariscope will show again that the fringes are bands and not lines. In both instances, the width of the fringes is due to the recording characteristics of the eye and the photographic film and not to inaccuracies in the previous development. If the intensity of light emerging from the analyzer is measured with a suitable photoelectric cell, a minimum intensity is recorded at some point near the center of the fringe which coincides with the exact extinction line.

C. Frequency Response of a Polariscope

The circular frequency ω for light in the visible spectrum is approximately 10^{15} rad/s. As a result, neither the eye nor any type of existing high-speed photographic equipment can detect the periodic extinction associated with the ωt term of the expression for the light wave. To date, no dynamic-stress problem has been attempted where the frequency response of the polariscope has proved inadequate. Instead, the problems encountered are associated with loading the model, recording the fringe pattern, and selecting a suitable model material.

13.6 EFFECTS OF A STRESSED MODEL IN A CIRCULAR POLARISCOPE (DARK FIELD, ARRANGEMENT A) [3, 8–12, 16, 17]

When a stressed photoelastic model is placed in the field of a circular polariscope with its normal coincident with the z axis of the polariscope, the optical effects differ somewhat from those obtained in a plane polariscope. The use of a circular polariscope eliminates the isoclinic fringe pattern while it maintains the isochromatic fringe pattern, and as a result the circular polariscope is more widely used than the plane polariscope. To illustrate this effect, consider the stressed model in the circular polariscope (arrangement A) shown in Fig. 13.7.

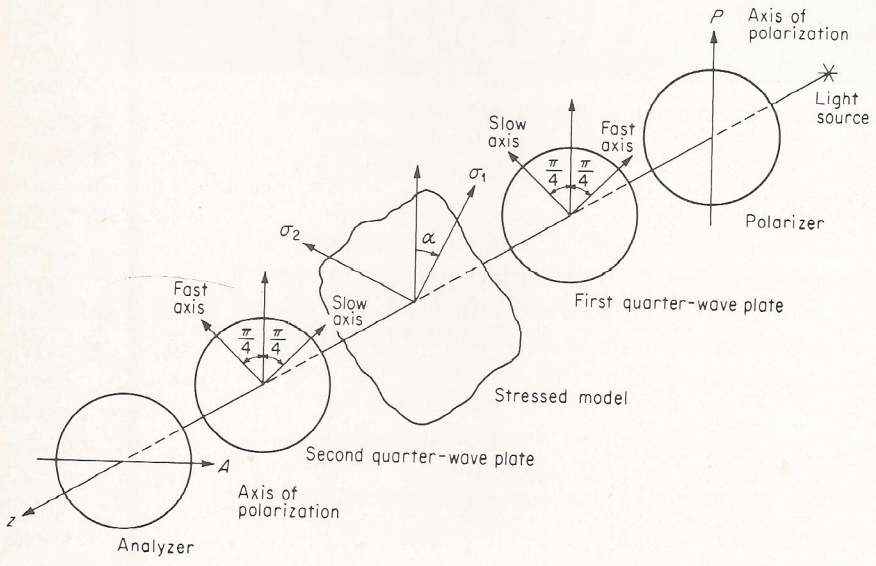

Figure 13.7 A stressed photoelastic model in a circular polariscope (arrangement A, crossed polarizer and analyzer, crossed quarter-wave plates).

The plane-polarized light beam emerging from the polarizer can be represented by the same simple expression used for the plane polariscope, namely,

$$E_{py} = k \cos \omega t \qquad (a)$$

As the light enters the first quarter-wave plate, it is resolved into components E_f and E_s with vibrations parallel to the fast and slow axes, respectively. Since the axes of the quarter-wave plate are oriented at 45° with respect to the axis of the polarizer,

$$E_f = \frac{\sqrt{2}}{2} k \cos \omega t \qquad E_s = \frac{\sqrt{2}}{2} k \cos \omega t$$

As the components propagate through the plate, they develop a relative angular phase shift $\Delta = \pi/2$; therefore, the components emerging from the plate can be expressed as

$$E'_f = \frac{\sqrt{2}}{2} k \cos \omega t \qquad E'_s = \frac{\sqrt{2}}{2} k \cos \left(\omega t - \frac{\pi}{2}\right) = \frac{\sqrt{2}}{2} k \sin \omega t \qquad (b)$$

It has previously been shown that these two plane-polarized beams represent circularly polarized light with the light vector rotating counterclockwise at any point along the axis of propagation of the light between the quarter-wave plate and the model.

After leaving the quarter-wave plate, the components enter the model in the manner illustrated in Fig. 13.8. Since the stressed model exhibits the character-

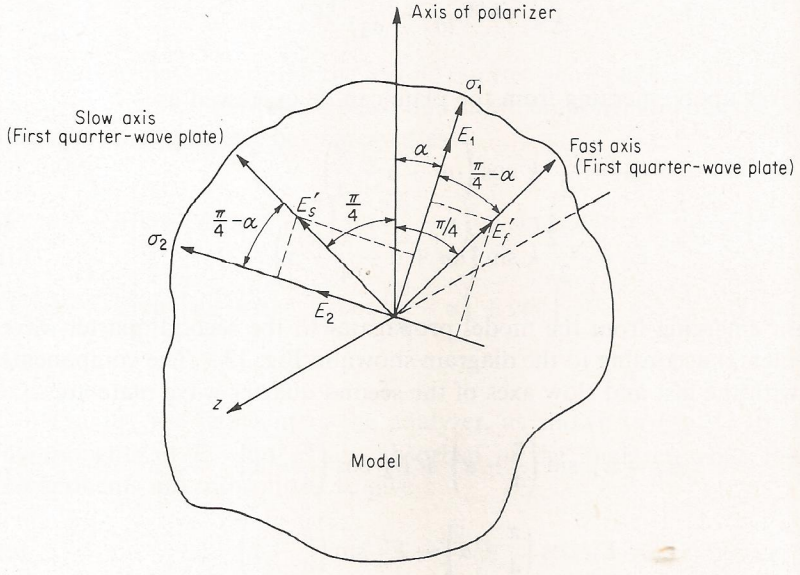

Figure 13.8 Resolution of the light components as they enter the stressed model.

istics of a temporary wave plate, the components E'_f and E'_s are resolved into components E_1 and E_2, which have directions of vibration parallel to the principal-stress directions in the model. Thus

$$E_1 = E'_f \cos\left(\frac{\pi}{4} - \alpha\right) + E'_s \sin\left(\frac{\pi}{4} - \alpha\right)$$

$$E_2 = E'_s \cos\left(\frac{\pi}{4} - \alpha\right) - E'_f \sin\left(\frac{\pi}{4} - \alpha\right) \qquad (c)$$

Substituting Eqs. (*b*) into (*c*) yields

$$E_1 = \frac{\sqrt{2}}{2} k \left[\cos \omega t \cos\left(\frac{\pi}{4} - \alpha\right) + \sin \omega t \sin\left(\frac{\pi}{4} - \alpha\right)\right]$$

$$= \frac{\sqrt{2}}{2} k \cos\left(\omega t + \alpha - \frac{\pi}{4}\right)$$

$$E_2 = \frac{\sqrt{2}}{2} k \left[\sin \omega t \cos\left(\frac{\pi}{4} - \alpha\right) - \cos \omega t \sin\left(\frac{\pi}{4} - \alpha\right)\right]$$

$$= \frac{\sqrt{2}}{2} k \sin\left(\omega t + \alpha - \frac{\pi}{4}\right)$$

The two components E_1 and E_2 propagate through the model with different velocities. The additional relative retardation Δ accumulated during passage through the model is given by Eq. (13.7) as

$$\Delta = \frac{2\pi hc}{\lambda}(\sigma_1 - \sigma_2)$$

Thus the waves upon emerging from the plate can be expressed as

$$E'_1 = \frac{\sqrt{2}}{2} k \cos\left(\omega t + \alpha - \frac{\pi}{4}\right)$$

$$E'_2 = \frac{\sqrt{2}}{2} k \sin\left(\omega t + \alpha - \frac{\pi}{4} - \Delta\right) \qquad (d)$$

The light emerging from the model propagates to the second quarter-wave plate and enters it according to the diagram shown in Fig. 13.9. The components associated with the fast and slow axes of the second quarter-wave plate are

$$E_f = E'_1 \sin\left(\frac{\pi}{4} - \alpha\right) + E'_2 \cos\left(\frac{\pi}{4} - \alpha\right)$$

$$E_s = E'_1 \cos\left(\frac{\pi}{4} - \alpha\right) - E'_2 \sin\left(\frac{\pi}{4} - \alpha\right) \qquad (e)$$

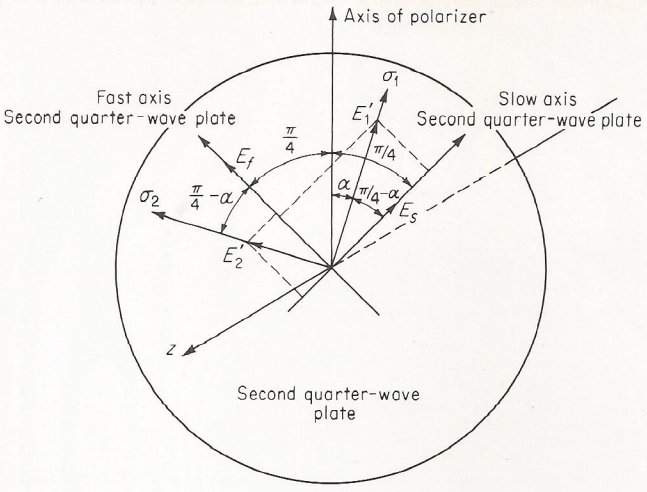

Figure 13.9 Resolution of the light components as they enter the second quarter-wave plate.

Substituting Eqs. (*d*) into (*e*) yields

$$E_f = \frac{\sqrt{2}}{2} k \left[\cos\left(\omega t + \alpha - \frac{\pi}{4}\right) \sin\left(\frac{\pi}{4} - \alpha\right) + \sin\left(\omega t + \alpha - \frac{\pi}{4} - \Delta\right) \cos\left(\frac{\pi}{4} - \alpha\right) \right]$$

$$E_s = \frac{\sqrt{2}}{2} k \left[\cos\left(\omega t + \alpha - \frac{\pi}{4}\right) \cos\left(\frac{\pi}{4} - \alpha\right) - \sin\left(\omega t + \alpha - \frac{\pi}{4} - \Delta\right) \sin\left(\frac{\pi}{4} - \alpha\right) \right]$$

As the light passes through the second quarter-wave plate, a relative phase shift of $\Delta = \pi/2$ develops between the fast and slow components. Thus the waves emerging from the plate can be expressed as

$$E_f' = \frac{\sqrt{2}}{2} k \left[\cos\left(\omega t + \alpha - \frac{\pi}{4}\right) \sin\left(\frac{\pi}{4} - \alpha\right) + \sin\left(\omega t + \alpha - \frac{\pi}{4} - \Delta\right) \cos\left(\frac{\pi}{4} - \alpha\right) \right]$$

$$E_s' = \frac{\sqrt{2}}{2} k \left[\sin\left(\omega t + \alpha - \frac{\pi}{4}\right) \cos\left(\frac{\pi}{4} - \alpha\right) + \cos\left(\omega t + \alpha - \frac{\pi}{4} - \Delta\right) \sin\left(\frac{\pi}{4} - \alpha\right) \right] \tag{13.16}$$

Finally, the light enters the analyzer, as shown in Fig. 13.10. The vertical components of E_f' and E_s' are absorbed in the analyzer while the horizontal components are transmitted to give

$$E_{ax} = \frac{\sqrt{2}}{2} (E_s' - E_f') \tag{f}$$

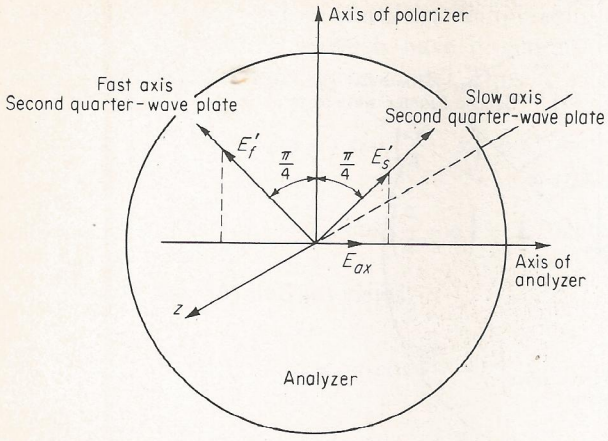

Figure 13.10 Components of the light vectors which are transmitted through the analyzer (dark field).

Substituting Eqs. (13.16) into Eq. (f) gives an expression for the light emerging from the analyzer of a circular polariscope (arrangement A). Thus

$$E_{ax} = \frac{k}{2}\left[\sin\left(\omega t + \alpha - \frac{\pi}{4}\right)\cos\left(\frac{\pi}{4} - \alpha\right) + \cos\left(\omega t + \alpha - \frac{\pi}{4} - \Delta\right)\sin\left(\frac{\pi}{4} - \alpha\right)\right.$$
$$\left. - \cos\left(\omega t + \alpha - \frac{\pi}{4}\right)\sin\left(\frac{\pi}{4} - \alpha\right) - \sin\left(\omega t + \alpha - \frac{\pi}{4} - \Delta\right)\cos\left(\frac{\pi}{4} - \alpha\right)\right]$$
$$= k \sin\frac{\Delta}{2}\sin\left(\omega t + 2\alpha - \frac{\Delta}{2}\right) \qquad (13.17)$$

Since the intensity of light is proportional to the square of the amplitude of the light wave, the light emerging from the analyzer of a circular polariscope (arrangement A) is given by

$$I = K \sin^2\frac{\Delta}{2} \qquad (13.18)$$

Inspection of Eq. (13.18) indicates that the intensity of the light beam emerging from the circular polariscope is a function only of the principal-stress difference since the angle α does not appear in the amplitude of the wave. This indicates that isoclinics have been eliminated from the fringe pattern observed with the circular polariscope. From the $\sin^2(\Delta/2)$ term in Eq. (13.18) it is clear that extinction will occur when $\Delta/2 = n\pi$, where $n = 0, 1, 2, 3, \ldots$. This type of extinction is identical with that previously described for the plane polariscope and referred to as an isochromatic fringe pattern. An example of this fringe pattern is shown in Fig. 13.11.

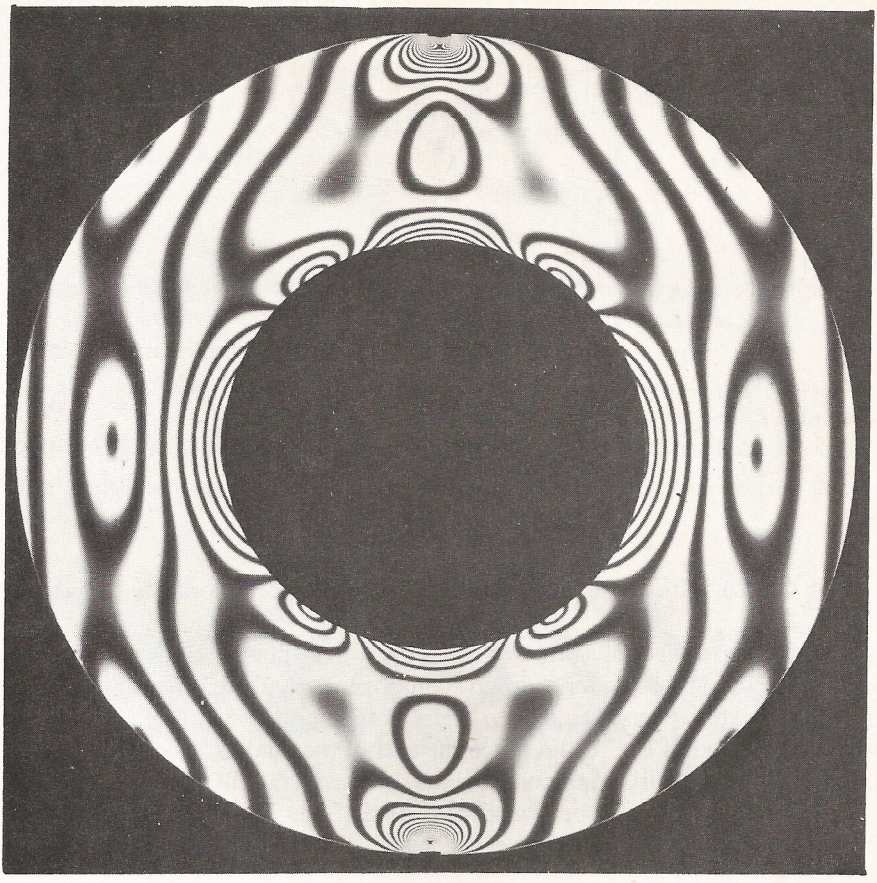

Figure 13.11 Dark-field isochromatic fringe pattern of a ring loaded in diametral compression.

13.7 EFFECTS OF A STRESSED MODEL IN A CIRCULAR POLARISCOPE (LIGHT FIELD, ARRANGEMENT B) [3, 8–12, 16, 17]

A circular polariscope is usually employed with both the dark- and light-field arrangements (*A* and *B*). The circular polariscope can be converted from dark field (arrangement *A*) to light field (arrangement *B*) simply by rotating the analyzer through 90°. The advantage of employing both light- and dark-field arrangements is that twice as many data are obtained for the whole-field determination of $\sigma_1 - \sigma_2$. Recall from Secs. 13.5 and 13.6 that the order of the fringes N coincides with n for the plane polariscope and for the dark-field circular polariscope; therefore, the fringes are counted in the sequence 0, 1, 2, 3, ... With the light-field arrangement of the circular polariscope, N and n do not coincide. Instead,

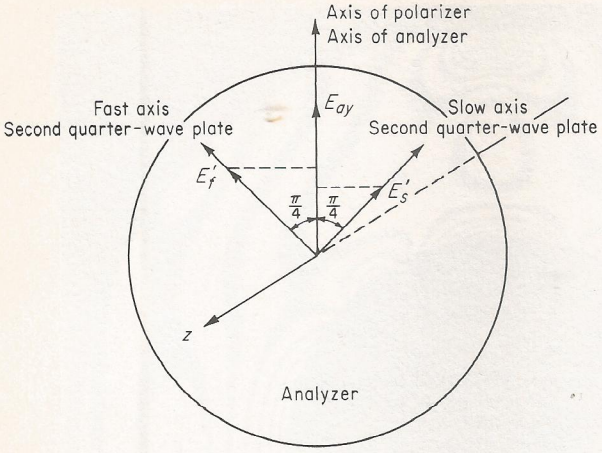

Figure 13.12 Components of the light vectors which are transmitted through the analyzer (light field).

$N = \frac{1}{2} + n$. Hence, with the light-field arrangement, the orders of the fringes are counted $\frac{1}{2}$, $1\frac{1}{2}$, $2\frac{1}{2}$, $3\frac{1}{2}$, ...

To establish the effect of a stressed model in a light-field circular polariscope, it is only necessary to consider the light components emerging from the second quarter-wave plate as represented by Eqs. (13.16) and the analyzer in its new position as indicated in Fig. 13.12. Since the axis of the analyzer is oriented in the vertical direction, the horizontal components of E'_f and E'_s will be absorbed while the vertical components will be transmitted as the light propagates through the analyzer. Thus, the emerging light vector, which lies in a vertical plane, can be expressed as

$$E_{ay} = \frac{\sqrt{2}}{2}(E'_s + E'_f) \tag{a}$$

Substituting Eqs. (13.16) into Eq. (*a*) yields

$$\begin{aligned} E_{ay} = \frac{k}{2}\Bigg[&\sin\left(\omega t + \alpha - \frac{\pi}{4}\right)\cos\left(\frac{\pi}{4} - \alpha\right) + \cos\left(\omega t + \alpha - \frac{\pi}{4} - \Delta\right)\sin\left(\frac{\pi}{4} - \alpha\right) \\ &+ \cos\left(\omega t + \alpha - \frac{\pi}{4}\right)\sin\left(\frac{\pi}{4} - \alpha\right) + \sin\left(\omega t + \alpha - \frac{\pi}{4} - \Delta\right)\cos\left(\frac{\pi}{4} - \alpha\right)\Bigg] \\ = k\cos\frac{\Delta}{2}&\sin\left(\omega t - \frac{\Delta}{2}\right) \end{aligned} \tag{13.19}$$

Since the intensity of light is proportional to the square of the amplitude of the light wave, the light emerging from the analyzer of a circular polariscope (arrangement *B*) is given by

$$I = K\cos^2\frac{\Delta}{2} \tag{13.20}$$

Equation (13.20) shows that extinction ($I = 0$) will occur when

$$\frac{\Delta}{2} = \frac{1 + 2n}{2}\pi \qquad \text{for } n = 0, 1, 2, 3, \ldots$$

or from Eq. (13.9) when

$$N = \frac{\Delta}{2\pi} = \frac{1}{2} + n$$

which implies that the order of the first fringe observed in a light-field polariscope is $\frac{1}{2}$, which corresponds to $n = 0$. An example of a light-field isochromatic fringe pattern is presented in Fig. 13.13.

By using the circular polariscope with both light- and dark-field arrangements, it is possible to obtain two photographs of the resulting isochromatic fringe patterns. The data thus obtained will give a whole-field representation of the order

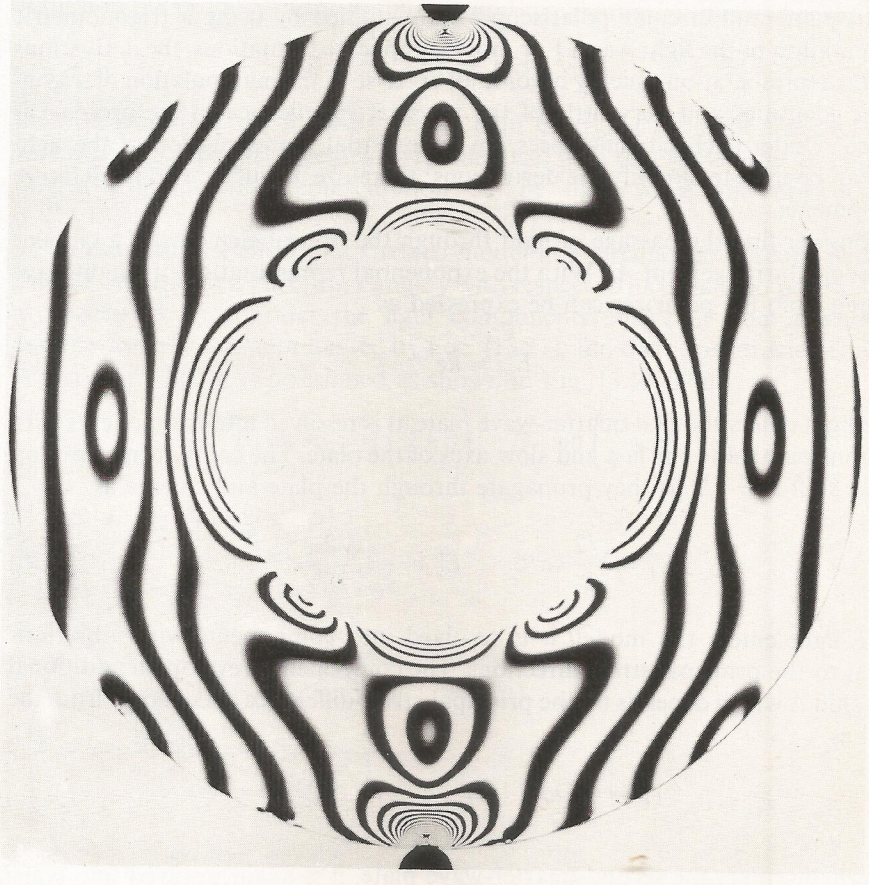

Figure 13.13 Light-field isochromatic fringe pattern of a ring loaded in diametral compression.

of the fringes to the nearest $\frac{1}{2}$ order. Interpolation between fringes often permits an estimate of the order of the fringes to ± 0.1, which results in accuracies for the principal-stress difference of $\pm 0.1 f_\sigma / h$. If more accurate determinations are necessary, the refined fringe-analysis techniques described in the following section can be used.

13.8 EFFECTS OF A STRESSED MODEL IN A CIRCULAR POLARISCOPE (ARBITRARY ANALYZER POSITION, TARDY COMPENSATION) [18–24]

The analysis presented in the previous two sections for the dark- and light-field arrangements of the circular polariscope can be carried one step further to include rotation of the analyzer through some arbitrary angle. The purpose of such a rotation is to provide a means for determining fractional fringe orders.

In the previous three sections, the optical effects produced by a stressed model in both plane and circular polariscopes were studied by using a trigonometric representation of the light wave. For more complicated situations, the derivations with this representation quickly become an exercise in the manipulation of trigonometric identities and very little of the physical significance of the problem is retained. Under such circumstances, an exponential representation of the light wave can be used to simplify the derivations; therefore, it will be used in all future developments.

Consider first the passage of light through the optical elements of a circular polariscope (arrangement *A*). With the exponential representation, the light wave emerging from the polarizer can be expressed as

$$E_{py} = k e^{i\omega t} \tag{a}$$

As the light enters the first quarter-wave plate, it is resolved into components with vibrations parallel to the fast and slow axes of the plate. The components develop a phase shift $\Delta = \pi/2$ as they propagate through the plate and emerge as

$$E'_f = \frac{\sqrt{2}}{2} k e^{i\omega t} \qquad E'_s = -i \frac{\sqrt{2}}{2} k e^{i\omega t} \tag{b}$$

As the light enters the model, it is resolved into components with vibrations parallel to the principal-stress directions. The components develop an additional phase shift Δ which depends on the principal-stress difference and emerge from the model as

$$E'_1 = \frac{\sqrt{2}}{2} k e^{i(\omega t + \alpha - \pi/4)} \qquad E'_2 = -i \frac{\sqrt{2}}{2} k e^{i(\omega t + \alpha - \pi/4 - \Delta)} \tag{c}$$

As the light enters the second quarter-wave plate, it is again resolved into components with vibrations parallel to the fast and slow axes of the plate. The com-

ponents experience a phase shift of $\Delta = \pi/2$ as they propagate through the plate and emerge as

$$E'_f = \frac{\sqrt{2}}{2}k\left[\sin\left(\frac{\pi}{4}-\alpha\right) - ie^{-i\Delta}\cos\left(\frac{\pi}{4}-\alpha\right)\right]e^{i(\omega t+\alpha-\pi/4)}$$

$$E'_s = \frac{\sqrt{2}}{2}k\left[e^{-i\Delta}\sin\left(\frac{\pi}{4}-\alpha\right) - i\cos\left(\frac{\pi}{4}-\alpha\right)\right]e^{i(\omega t+\alpha-\pi/4)} \qquad (13.21)$$

Finally, as the light passes through the analyzer, the vertical components of E'_f and E'_s are absorbed while the horizontal components are transmitted. Thus

$$E_{ax} = \frac{k}{2}\left[(e^{-i\Delta}-1)\sin\left(\frac{\pi}{4}-\alpha\right) + i(e^{-i\Delta}-1)\cos\left(\frac{\pi}{4}-\alpha\right)\right]e^{i(\omega t+\alpha-\pi/4)}$$

$$= \frac{k}{2}(e^{-i\Delta}-1)e^{i(\omega t+2\alpha)} \qquad (13.22)$$

Recall from Eq. (11.17) that the square of the amplitude of a wave in exponential notation is the product of the amplitude and its complex conjugate. Thus

$$I \propto E_{ax}E^*_{ax} = K\sin^2\frac{\Delta}{2} \qquad (13.23)$$

This expression for the intensity of the light emerging from the analyzer of a circular polariscope (arrangement *A*) is identical with that previously determined using a trigonometric representation of the light wave and presented in Eq. (13.18).

To establish the effect of a stressed model in a circular polariscope with the analyzer oriented at an arbitrary angle γ with respect to its dark-field position, it is only necessary to consider the light components emerging from the second quarter-wave plate, as represented by Eqs. (13.21), and their transmission through the analyzer when it is positioned as shown in Fig. 13.14. Thus

$$E_{a\gamma} = E'_s\cos\left(\frac{\pi}{4}+\gamma\right) - E'_f\sin\left(\frac{\pi}{4}+\gamma\right) \qquad (d)$$

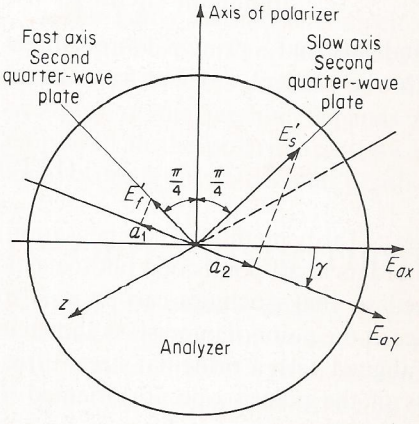

Figure 13.14 Rotation of the analyzer to obtain extinction in the Tardy method of compensation.

Substituting Eqs. (13.21) into Eq. (d) and combining terms yields

$$E_{a\gamma} = \frac{\sqrt{2}}{2} k \left\{ \sin\left(\frac{\pi}{4} - \alpha\right) \left[e^{-i\Delta} \cos\left(\frac{\pi}{4} + \gamma\right) - \sin\left(\frac{\pi}{4} + \gamma\right) \right] + i \cos\left(\frac{\pi}{4} - \alpha\right) \left[e^{-i\Delta} \sin\left(\frac{\pi}{4} + \gamma\right) - \cos\left(\frac{\pi}{4} + \gamma\right) \right] \right\} e^{i(\omega t + \alpha - \pi/4)} \tag{13.24}$$

The intensity of the light emerging from the analyzer is given by Eq. (11.17) as

$$I \propto E_{a\gamma} E_{a\gamma}^* \tag{e}$$

Substituting Eq. (13.24) and its complex conjugate into Eq. (e) and combining terms through the use of suitable trigonometric identities yields

$$I = K(1 - \cos 2\gamma \cos \Delta - \cos 2\alpha \sin 2\gamma \sin \Delta) \tag{13.25}$$

For a given angle of analyzer rotation γ, values of α and Δ required for maximum intensity or minimum intensity are obtained from

$$\frac{\partial I}{\partial \alpha} = K(2 \sin 2\alpha \sin 2\gamma \sin \Delta) = 0 \tag{f}$$

$$\frac{\partial I}{\partial \Delta} = K(\cos 2\gamma \sin \Delta - \cos 2\alpha \sin 2\gamma \cos \Delta) = 0 \tag{g}$$

Values of α and Δ satisfying Eqs. (f) and (g) simultaneously are

$$\alpha = \begin{cases} \dfrac{(2n+1)\pi}{4} \\ \\ \dfrac{n\pi}{2} \end{cases} \quad \text{and} \quad \Delta = \begin{cases} n\pi & n = 0, 1, 2, 3, \ldots \\ & \text{maximum intensity} \\ 2\gamma \pm 2n\pi & n = 0, 1, 2, 3, \ldots \\ & \text{minimum intensity} \end{cases}$$

The above conditions for extinction ($I = 0$) indicate that a principal-stress direction must be parallel to the axis of the polarizer ($\alpha = 0, \pi/2, \ldots$). The fringe order at the point is then

$$N = \frac{\Delta}{2\pi} = n \pm \frac{\gamma}{\pi} \tag{13.26}$$

Rotation of the analyzer through an angle γ (Tardy method of compensation) is widely used to determine fractional fringe orders at all points of a photoelastic model. A plane polariscope is first employed so that isoclinics can be used to establish the directions of the principal stresses at the point of interest, as shown in Fig. 13.15. The axis of the polarizer is then aligned with a principal-stress direction ($\alpha = 0$ or $\pi/2$), and the other elements of the polariscope are oriented to

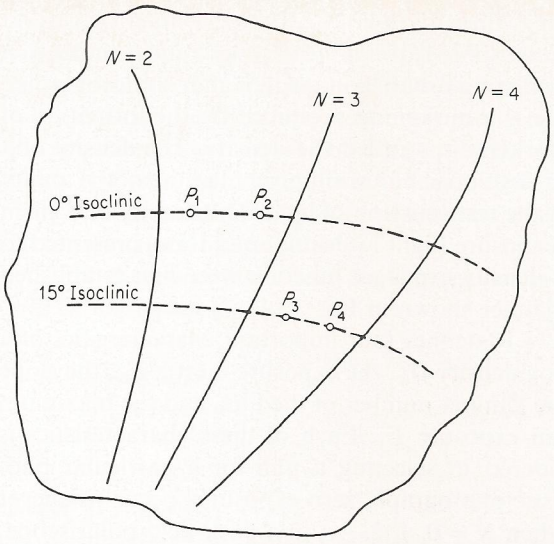

Figure 13.15 Locations of the points of interest relative to the dark-field isochromatic fringe pattern.

produce a standard dark-field circular polariscope. The analyzer is then rotated until extinction occurs at the point of interest, as indicated by Eq. (13.26). To illustrate the procedure, consider the hypothetical dark-field fringe pattern and points of interest shown in Fig. 13.15. At point P_1, which lies between fringes of orders 2 and 3, the value assigned to n is 2. As the analyzer is rotated through an angle γ, the second-order fringe will move toward point P_1 until extinction is obtained. The fringe order at P_1 is then given by $N = 2 + \gamma/\pi$. For point P_2 the value of n is also taken as 2, and the analyzer is rotated through an angle γ_1 until the second-order fringe produces extinction, giving a value for the fringe order of $N = 2 + \gamma_1/\pi$. In this instance n could also be taken as 3, and the analyzer rotated in the opposite direction through an angle $-\gamma_2$ until the third-order fringe produced extinction at point P_2. In this instance the fringe order would be given by $N = 3 - \gamma_2/\pi$, which should check the value of $N = 2 + \gamma_1/\pi$ obtained previously.

The Tardy method of compensation can be quickly and effectively employed to determine fractional fringe orders at arbitrary points in a model, provided isoclinic parameters are used to obtain the directions of the principal stresses. The accuracy of the method depends upon the quality of the quarter-wave plates employed in the polariscope; however, fringe orders obtained with this method and accurate to two decimal points are often quoted in the literature.

13.9 PHOTOELASTIC PHOTOGRAPHY [25, 26]

In most photoelastic analyses, photographs are taken of the isochromatic and isoclinic fringe patterns to establish a permanent record of the test. For this reason it is important that the basic principles of photography be established and that the differences between landscape and photoelastic photography be understood.

A sheet of photographic film is prepared with a coating containing certain silver halides. When this coating is exposed to light, the silver halides undergo a latent change that is permanently distinguishable on the film after a photographic development process. The change is a darkening produced by the formation of metallic silver. The amount of darkening is called the density. The density of a portion of a piece of exposed and developed film is simply a measure of the ability of the deposited silver to prevent the transmission of light. The density of a given type of film is a function of the exposure (light intensity times time) presented to the film. The characteristics of a density-exposure function were first established by Hurter and Driffield in the manner shown in Fig. 13.16.

The curve presented in Fig. 13.16 defines four important characteristics of a photographic film; namely, the fog density D_0, the exposure inertia E_0, the slope of the curve which establishes the gamma number of the film, and the maximum density D_1 which occurs with an exposure E_1. Each of these characteristics is important and should be considered in selecting a film for a particular photoelastic analysis. In a photoelastic photograph, zero exposures occur whenever the intensity goes to zero, i.e., when $N = 0, 1, 2, \ldots$, in a dark-field polariscope; however, the film coating records values of the ranges of exposure above the inertia value E_0. It is this "dead" exposure which produces the fringe width on a negative when in theory the fringe is a line. The slope of the density-versus-log-exposure curve given by γ determines the latitude of the film. The usual landscape film incorporates an emulsion with $\gamma \approx 1$. This relatively low value of γ gives a wide range of exposure values over which the film emulsion will be effective in producing a satisfactory negative. This feature is of course important in landscape photography, where the proper exposure time cannot be precisely established. For photoelastic photographs, film emulsions with a high γ (3 to 6) are often employed

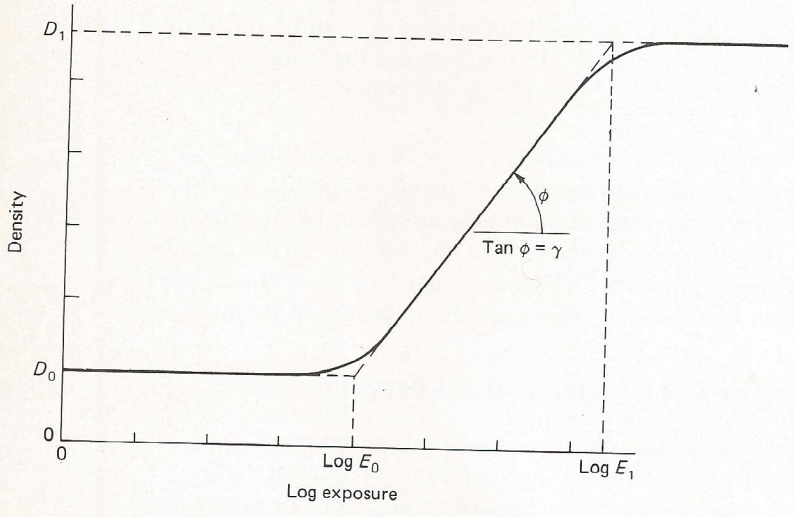

Figure 13.16 Hurter-Driffield graph relating exposure and density.

since this type of film gives a high-contrast negative; i.e., blacks are very black, whites are very white, with very little gray. This is a desirable situation since the fringes tend to sharpen and become better defined. The exposure time is of course more critical, but this time can be accurately established in preliminary exposures for any given polariscope. The fog density D_0 is less important since it implies that there is a thin coating uniformly distributed over the film which absorbs light. This of course detracts from the sharpness of a negative, but since it is a relative factor it is not objectionable.

For the linear portion of the density-versus-log-exposure curve, the density D can be expressed as

$$D = \begin{cases} D_0 + \gamma(\log E - \log E_0) & \text{for } E_0 \leq E \leq E_1 \\ D_0 & \text{for } E \leq E_0 \\ D_1 & \text{for } E \geq E_1 \end{cases} \tag{13.27}$$

where $D = \log I_i/I_e$
I_i = intensity of light incident upon developed negative
I_e = intensity of light emerging from developed negative
D_0 = fog density = $\log I_i/I_{e'}$
D_1 = maximum density = $\log I_i/I_{e''}$
$I_{e'}$ = intensity of light emerging from the unexposed part of developed negative
$I_{e''}$ = intensity of light emerging from an overexposed part of developed negative
$E = It$
I = intensity of light incident on film
t = time of exposure

By employing the above definitions, Eq. (13.27) can be rewritten as

$$\log \frac{I_i}{I_e} = \log \frac{I_i}{I_{e'}} + \gamma \log \frac{E}{E_0} \tag{a}$$

which can be reduced to

$$\rho = \frac{I_e}{I_{e'}} = \left(\frac{E}{E_0}\right)^{-\gamma} \qquad \text{for } E_1 \geq E \geq E_0 \tag{13.28}$$

where ρ is called the brightness ratio = $I_e/I_{e'}$. From this definition it follows that $\rho = 1$ corresponds to the brightest area on the negative, while $\rho = 0$ corresponds to an opaque area. Note that $\rho = 1$ when $E \leq E_0$ since $I_e = I_{e'}$ and that $\rho \to 0$ when $E \geq E_1$ since $I_e = I_{e''}$.

Now recall Eq. (13.18), where the light intensity produced by inserting a stressed model in a circular polariscope is given by

$$I = K \sin^2 \frac{\Delta}{2} \tag{13.18}$$

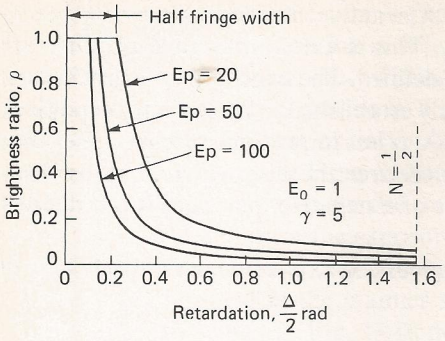

Figure 13.17 Brightness ratio as a function of retardation.

The exposure for the dark-field negative will be

$$E = It = Kt \sin^2 \frac{\Delta}{2} = E_p \sin^2 \frac{\Delta}{2} \tag{13.29}$$

where $E_p = Kt$ is the uniform exposure produced by the polariscope. Combining Eqs. (13.28) and (13.29) gives

$$\rho \begin{cases} = \dfrac{1}{(E_p/E_0)^{\gamma} \sin^{2\gamma}(\Delta/2)} & \text{for } E_1 \geq E_p \sin^2 \dfrac{\Delta}{2} \geq E_0 \\ = 1 & \text{for } E_p \sin^2 \dfrac{\Delta}{2} \leq E_0 \\ \to 0 & \text{for } E_p \sin^2 \dfrac{\Delta}{2} \geq E_1 \end{cases} \tag{13.30}$$

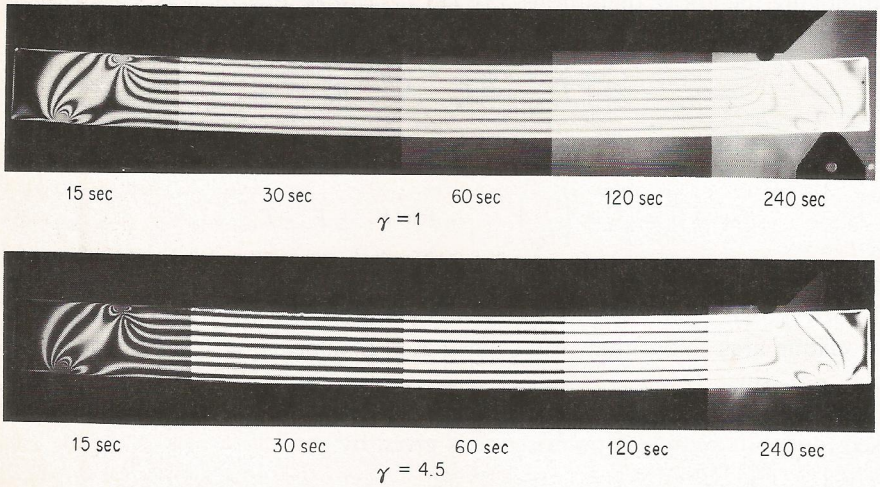

Figure 13.18 Influence of exposure time and gamma number on the appearance of the isochromatic fringe pattern for a beam in pure bending.

The results of Eqs. (13.30) describe the brightness ratio ρ for a dark-field photoelastic photograph. An example of the variation of ρ with $\Delta/2$ is given in Fig. 13.17 for three different exposures ($E_p/E_0 = 20$, 50, and 100). It should be noted that increasing the exposure ratio E_p/E_0 reduces the fringe width and improves the contrast. This sharpening of the fringes by increasing the exposure time is illustrated in Fig. 13.18 for both high-contrast and landscape film.

13.10 FRINGE MULTIPLICATION BY PHOTOGRAPHIC METHODS [27, 28]

By employing normal photoelastic procedures, two photographs (one light-field, the other dark-field) are obtained which permit the determination of the order of the fringes in the following sequence: $N = 0, \frac{1}{2}, 1, 1\frac{1}{2}, 2, 2\frac{1}{2}, \ldots$. In certain photoelastic applications it is desirable to improve the accuracy of the determination of fractional fringe orders which are between those previously listed. This objective can be accomplished in a number of ways. In this section a photographic technique is described which gives, through superposition of ordinary light- and dark-field isochromatic fringe patterns, a new fringe pattern (mixed-field). This mixed-field pattern has fringes at the $N/4$ and $3N/4$ positions. Use of the mixed-field fringe pattern coupled with ordinary light- and dark-field fringe patterns permits the orders of the fringes to be determined in the $0, \frac{1}{4}, \frac{1}{2}, \frac{3}{4}, 1, \frac{5}{4}, \ldots$ sequence, and thus represents a factor of 2 increase in the number of countable fringes.

The proof of this photographic method can easily be established by drawing from the results established in Secs. 13.6, 13.7, and 13.9. From Eqs. (13.30), which describe the brightness of a negative obtained with a dark-field polariscope,

$$\rho_d \begin{cases} = \dfrac{1}{(E_{pd}/E_0)^\gamma \sin^{2\gamma}(\Delta/2)} & \text{for } E_1 \geq E_{pd} \sin^2 \dfrac{\Delta}{2} \geq E_0 \qquad (a) \\ = 1 & \text{for } E_{pd} \sin^2 \dfrac{\Delta}{2} \leq E_0 \qquad (b) \\ \to 0 & \text{for } E_{pd} \sin^2 \dfrac{\Delta}{2} \geq E_1 \qquad (c) \end{cases}$$

Similarly by combining Eqs. (13.28) and (13.29) with Eq. (13.20), the brightness ratio for a negative in a light-field polariscope is

$$\rho_l \begin{cases} = \dfrac{1}{(E_{pl}/E_0)^\gamma \cos^{2\gamma}(\Delta/2)} & \text{for } E_1 \geq E_{pl} \cos^2 \dfrac{\Delta}{2} \geq E_0 \qquad (d) \\ = 1 & \text{for } E_{pl} \cos^2 \dfrac{\Delta}{2} \leq E_0 \qquad (e) \\ \to 0 & \text{for } E_{pl} \cos^2 \dfrac{\Delta}{2} \geq E_1 \qquad (f) \end{cases}$$

The effect of superimposing light and dark field negatives is obtained by multiplying the expressions for the brightness ratios. Thus, the brightness ratio ρ_m for the mixed field associated with superimposed light- and dark-field negatives is

$$\rho_m = \rho_d \rho_l \tag{g}$$

Equation (g) leads to four nonzero expressions for ρ_m

$$\rho_m = \begin{cases} 1 & \text{from Eqs. } (b) \text{ and } (e) \\ \dfrac{1}{(E_{pl}/E_0)^\gamma \cos^{2\gamma}(\Delta/2)} & \text{from Eqs. } (b) \text{ and } (d) \\ \dfrac{1}{(E_{pd}/E_0)^\gamma \sin^{2\gamma}(\Delta/2)} & \text{from Eqs. } (a) \text{ and } (e) \\ \dfrac{1}{(E_{pd}/E_0)^\gamma (E_{pl}/E_0)^\gamma \sin^{2\gamma}(\Delta/2) \cos^{2\gamma}(\Delta/2)} & \text{from Eqs. } (a) \text{ and } (d) \end{cases}$$

Of these four solutions for ρ_m, the solution $\rho_m = 1$ locates the fringe position on the superimposed negative. Note that $\rho_m = 1$ only in regions where both

$$\cos^2 \frac{\Delta}{2} \leq \frac{E_0}{E_{pl}} \qquad \text{and} \qquad \sin^2 \frac{\Delta}{2} \leq \frac{E_0}{E_{pd}} \tag{h}$$

With equal light- and dark-field exposures

$$E_{pd} = E_{pl} = ME_0 \tag{i}\dagger$$

where M is the exposure multiple. Combining Eqs. (h) and (i) yields the condition $M \leq 2$ to obtain any region on the superimposed negative where $\rho_m = 1$. With $M = 2$, Eqs. (h) become

$$\cos^2 \frac{\Delta}{2} \leq \frac{1}{2} \qquad \sin^2 \frac{\Delta}{2} \leq \frac{1}{2} \tag{13.31}$$

It is evident then that

$$\frac{\Delta}{2} = \frac{(2n+1)\pi}{4} \qquad \text{where } n = 0, 1, 2, 3, \ldots$$

and

$$N = \frac{\Delta}{2\pi} = \frac{2n+1}{4} \tag{13.32}$$

With $E_{pd} = E_{pl}$ and $M = 2$, the superimposed negatives yield a fringe pattern where the $\frac{1}{4}$-order fringes are displayed with $N = \frac{1}{4}, \frac{3}{4}, \frac{5}{4}, \ldots$. A schematic illustration of the brightness ratio ρ_m as a function of retardation $\Delta/2$ is shown in Fig. 13.19.

† A more general treatment of exposure ratio leads to a whole-field compensation technique [32–34].

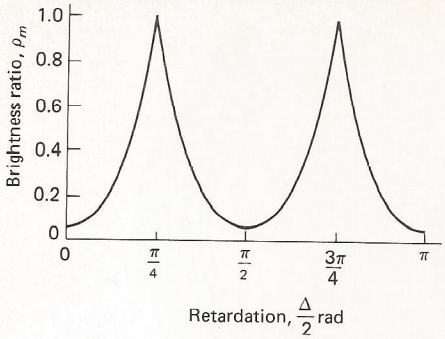

Figure 13.19 Mixed-field brightness ratio as a function of retardation.

The photographic method of fringe multiplication (doubling) is illustrated in the two examples cases presented below.

Beam subjected to a constant moment The model of the beam was machined from $\frac{1}{4}$-in-thick CR-39, and a constant moment was applied to the central portion of the beam by employing the four-point loading technique. Lines were scribed on the model in order to permit easier alignment of the two negatives during superposition. The load was increased so that in the region of constant moment there were about four fringes. So that the photographic method of superposition of negatives could be carried out, the exposure was kept low. With Kodak contrast-process panchromatic films, an aperture setting f: 45, and an exposure time of 15 s, light- and dark-field photographs were taken. The contrast-process film used for this and all the subsequent experiments was developed for 6 min in Kodak D-11 developer. On superposition of light- and dark-field negatives, it was found that the fringes were distinct and of uniform intensity. If the exposure time was greater than the optimum value ($M = 2$), the uniform exposure of the two negatives became prohibitively high and light would not pass through the two negatives. Employing exposures under the optimum value produced films so thin that the fringes were not well defined upon superposition of the negatives. The fringe patterns obtained for the light field, dark field, and superimposed or mixed fields are shown in Fig. 13.20.

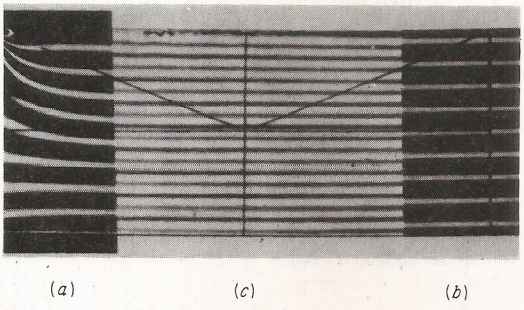

Figure 13.20 (*a*) Dark-, (*b*) light-, and (*c*) mixed-field isochromatic fringe patterns of a beam subjected to a constant binding moment.

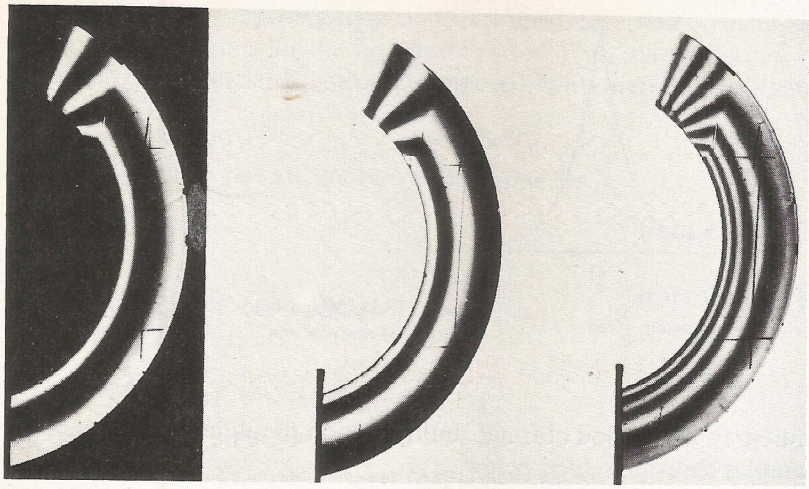

(a) (b) (c)

Figure 13.21 (*a*) Dark-, (*b*) light-, and (*c*) mixed-field isochromatic fringe patterns from a three-dimensional slice.

Slice from a three-dimensional model The model was a segment of a hoop slice taken from a thick-walled pressure vessel subjected to internal pressure. One end of the segment was machined into the shape of a wedge in order to locate the zero-order fringe. The slice was polished and mounted in the field of the polariscope, and light- and dark-field photographs were taken. The dark-, light-, and mixed-field photographs shown in Fig. 13.21 illustrate the improvement possible in the fringe-order determination by employing this fringe-doubling technique.

13.11 FRINGE SHARPENING WITH PARTIAL MIRRORS [29]

The bandwidth of the isochromatic fringe can be reduced by a novel technique due to Post [29], which employs partial mirrors† in a circular-lens polariscope. The partial mirrors are inserted into the field of the polariscope on both sides of the model and parallel to it, as illustrated in Fig. 13.22.

The effect of the partial mirrors is to cause the light to propagate back and forth through the model in the manner illustrated in Fig. 13.23. As the light is reflected back and forth between the two mirrors, a portion of it is transmitted at each reflection point. Hence, the intensity of the ray passing back and forth through the model is progressively decreasing. For instance, ray 1 is the most intense, ray 3 less intense, etc. The rays shown in Fig. 13.23 are drawn obliquely

† A partial mirror, sometimes called a *beam splitter*, is simply an optical element that transmits a portion of the incident light and reflects the remainder so that $T + R = 1$, where T is the coefficient of transmission and R is the coefficient of reflection.

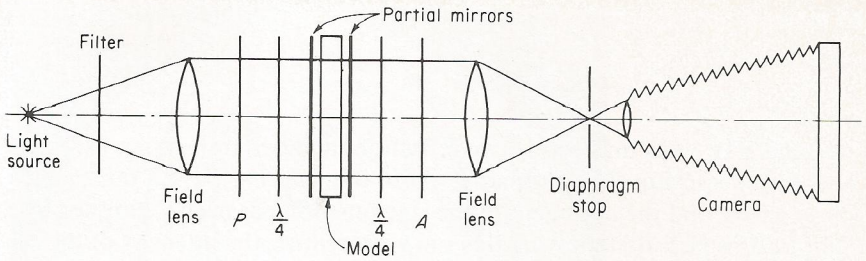

Figure 13.22 Post's modification of the lens polariscope, with partial mirrors for fringe sharpening.

only to present the effects of the partial mirrors; in practice, normal incidence is employed and all the rays coincide and enter and emerge from the same point in the model.

The effect of the partial mirrors on the intensity of the light as it passes through a stressed model can be obtained by modifying Eq. (13.18), which is valid if no partial mirrors are employed in the polariscope:

$$I = K \sin^2 \frac{\Delta}{2} \tag{13.18}$$

Consider ray 1 (see Fig. 13.23) and reduce the intensity due to the light lost by reflection from the partial mirrors at points A and B. Thus

$$I_1 = K(1 - R)^2 \sin^2 \frac{\Delta}{2} = KT^2 \sin^2 \frac{\Delta}{2} \tag{a}$$

where R and T are the reflection and transmission coefficients of the partial mirror.

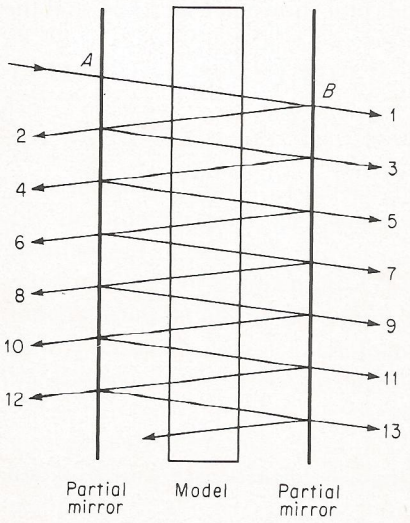

Figure 13.23 Light reflection and transmission between two partial mirrors.

The intensity of the light associated with ray 3 can be written as

$$I_3 = KT^2R^2 \sin^2 \frac{3\Delta}{2} \tag{b}$$

In this instance ray 3 has undergone two reflections and two transmissions; hence the T and R terms in Eq. (*b*) are squared. Also, the light has passed through the model three times, and the argument of the sine function has been multiplied by 3 to account for this fact. By following this same procedure, the intensity of the kth ray may be written as

$$I_k = KT^2R^{k-1} \sin^2 \frac{k\Delta}{2} \qquad k = 1, 3, 5, 7, \ldots \tag{13.33}$$

These intensities $I_1, I_3, I_5, \ldots, I_k$ add arithmetically; hence the resultant intensity of the superimposed rays is given by the series expansion

$$I = KT^2 \sum_{k=1}^{\prime} R^{k-1} \sin^2 \frac{k\Delta}{2} \tag{13.34}$$

If this relationship is expanded and plotted as a function of $\Delta/2\pi = N$, the intensity-versus-fringe-order plot shown in Fig. 13.24 is obtained. When this plot is compared with the conventional intensity-versus-$\Delta/2$ plot, also shown in Fig. 13.24, it is clear why the fringes are sharpened. The eye will begin to record a fringe at some minimum intensity I_0; hence the sharpened intensity function produces a much narrower fringe than the conventional intensity function. An example of the isochromatic fringe pattern produced with a pair of partial mirrors, each with a reflection coefficient $R = 0.9$ and a transmission coefficient $T = 0.1$, is shown in Fig. 13.25.

An examination of this figure shows that the sharp light and dark fringes observed are separated by wide gray bands. The dark fringes correspond to the sharp valleys on the intensity-versus-fringe-order plot shown in Fig. 13.24, and the

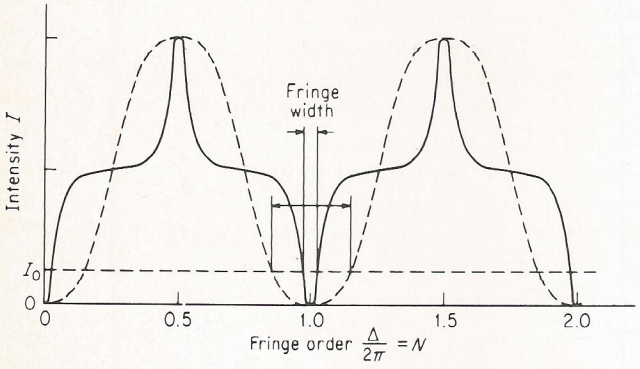

Figure 13.24 Intensity as a function of fringe order in a standard circular polariscope with partial mirrors where $R = 0.85$. (*Courtesy of D. Post.*)

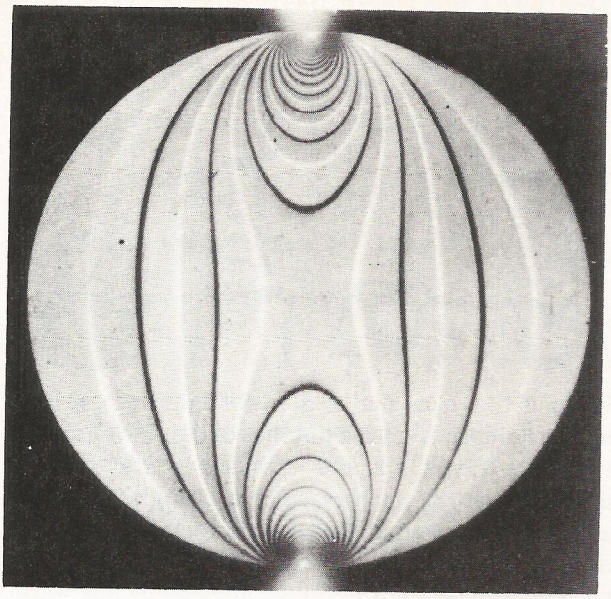

Figure 13.25 Isochromatic fringe pattern produced by a dark-field circular polariscope equipped with partial mirrors. (*Courtesy of D. Post.*)

light fringes correspond to the sharp peaks on this same graph. The wide gray bands are produced by the midrange of intensity also shown in this figure. The dark fringes are ordered in a 0, 1, 2, 3, ... sequence, and the light fringes are ordered in the $\frac{1}{2}$, $1\frac{1}{2}$, $2\frac{1}{2}$, $3\frac{1}{2}$, ... sequence. Thus, the data normally obtained from two conventional light- and dark-field photographs are contained in one photograph if partial mirrors are employed in the standard circular lens polariscope.

13.12 FRINGE MULTIPLICATION WITH PARTIAL MIRRORS [29–31]

Post has also shown that partial mirrors can be quite usefully employed to multiply the number of fringes which can be observed in a photoelastic model. As pointed out in Sec. 13.8, fringe multiplication is quite important since the standard methods of compensation used to evaluate the fractional fringe orders are time-consuming and in certain cases somewhat inaccurate. Fringe multiplication is, in a sense, a whole-field compensation technique where the fractional orders of the fringes can be determined simultaneously at all points on the model.

When partial mirrors are used in fringe multiplication, they are again inserted into a lens polariscope on both sides of the model; however, in this application one of the mirrors is inclined slightly, as illustrated in Fig. 13.26. The effect of the inclined partial mirror on the light passing back and forth through the model is

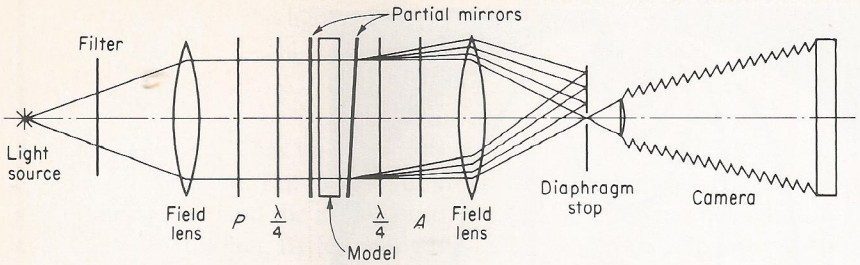

Figure 13.26 Partial mirrors as employed in a circular-lens polariscope for fringe multiplication.

shown in Fig. 13.27. From this figure it is clear that each ray of light emerges from the mirror system at an angle which depends on the number of times the light ray has traversed the model. For instance, rays 1, 3, 5, and 7, which have traversed the model the same number of times as their ray number, emerge at angles 0, 2ϕ, 4ϕ, and 6ϕ. Although the rays do not pass through the same point, the inclination angle ϕ used in the illustration was greatly exaggerated. The length of the line over which the photoelastic effect is averaged depends upon the angle of inclination ϕ, the ray number, and the separation distance between the mirrors. In practice, multiplication by factors of 5 to 7 can be achieved without introducing objectionable errors due to the averaging process which is inherent in this method. Typical patterns obtained from a two-dimensional model and from a three-dimensional slice are illustrated in Figs. 13.28 and 13.29.

The fact that different rays of light are inclined at different angles with respect to the axis of the polariscope permits each ray to be isolated. The rays are all

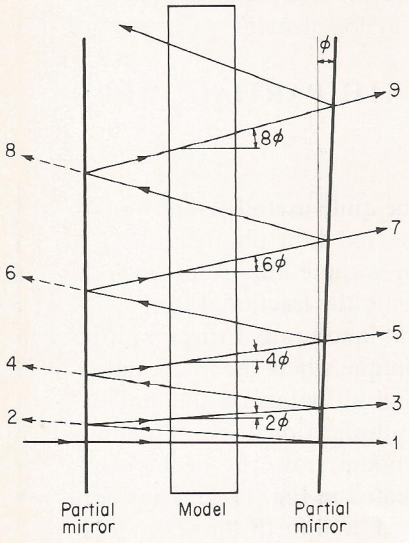

Figure 13.27 Light reflection and transmission between two slightly inclined partial mirrors.

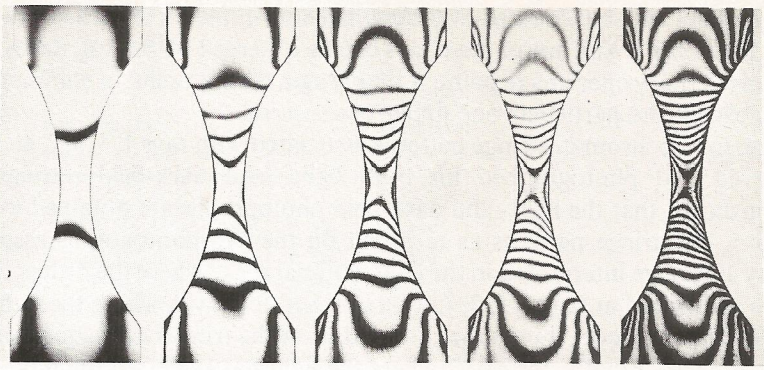

Figure 13.28 Isochromatic fringe patterns of a tensile specimen obtained by using a lens polariscope equipped with partial mirrors. (*Polarizing Instrument Company.*)

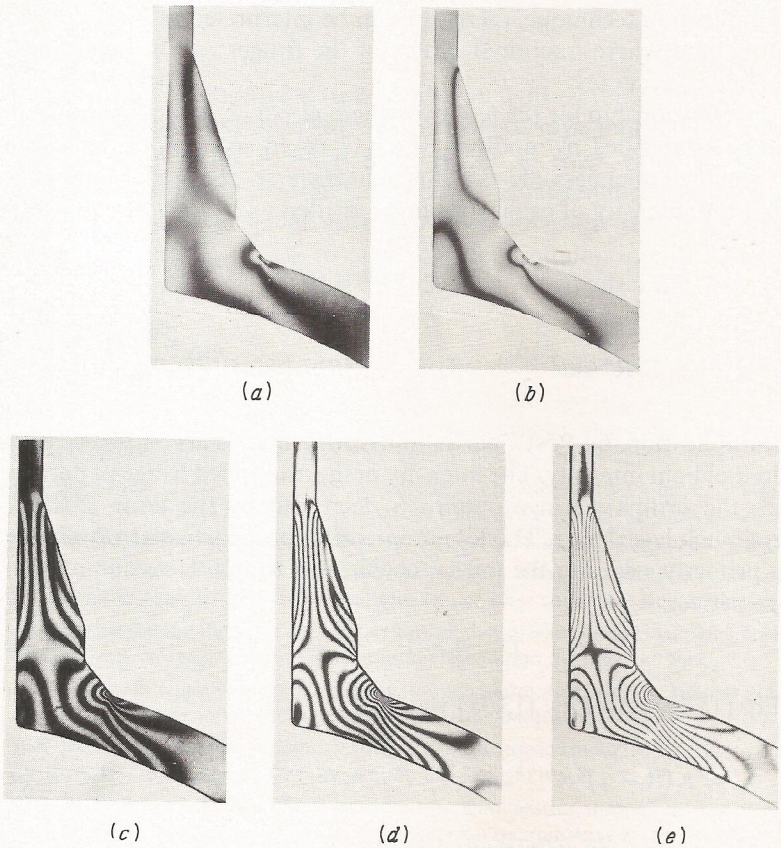

Figure 13.29 Isochromatic fringe patterns of a three-dimensional slice obtained by using a lens polariscope equipped with partial mirrors: (*a*) normal fringe pattern; (*b*) sharpened fringe pattern; (*c*) after fringe multiplication 3X; (*d*) after fringe multiplication 5X; (*e*) after fringe multiplication 7X. (*Courtesy of C. E. Taylor.*)

collected by the field lens but focused at different points in the focal plane of the field lens (see Fig. 13.26). Any one of these rays can be observed by placing the eye or a camera lens at the proper image point. A diaphragm stop is useful in eliminating all images except the particular one under observation.

In practice, the isochromatic fringe patterns associated with rays 1, 3, 5, 7, etc., can be observed and photographed for both light- and dark-field settings. Suppose, for instance, that the light- and dark-field photographs are obtained for rays 1, 3, and 5. The fringe patterns as recorded on the two photographs associated with ray 1 may be interpreted in the conventional sense where the orders of the fringes are sequenced as $0, \frac{1}{2}, 1, \frac{3}{2}, 2, \frac{5}{2}, \ldots$. However, for ray 3, where the light has passed through the model three times, the orders of the fringes are sequenced as $0, \frac{1}{6}, \frac{1}{3}, \frac{1}{2}, \frac{2}{3}, \frac{5}{6}, 1, \ldots$. Finally, for ray 5, where the light has traversed the model five times, the orders of the fringes are sequenced as $0, \frac{1}{10}, \frac{1}{5}, \frac{3}{10}, \frac{2}{5}, \frac{1}{2}, \ldots$. Thus the superposition of the results obtained from these three rays is sufficient to determine the fringe order to the nearest one-tenth of an order over the entire model. The fringe-multiplication technique, therefore, can be interpreted as a whole-field compensation method where fractional orders of the fringes can be determined with a high degree of accuracy.

The intensity relationship for the mth ray, where $m = 1, 2, 3, 4, 5$, as shown in Fig. 13.27, can be established by modifying Eq. (13.18) to account for the loss in intensity and the added thickness effects as the light traverses the model m times. It is apparent that the intensity of each ray can be written as

$$I_1 = KT^2 \sin^2 \frac{\Delta}{2} \qquad I_3 = KT^2R^2 \sin^2 \frac{3\Delta}{2}$$

$$I_5 = KT^2R^4 \sin^2 \frac{5\Delta}{2} \qquad I_m = KT^2R^{m-1} \sin^2 \frac{m\Delta}{2} \tag{13.35}$$

Thus, fringe multiplication, by Post's partial-mirror method, is accompanied by a considerable loss of light intensity. The intensity of the multiplied fringe pattern as compared with the ordinary fringe pattern is decreased by the term T^2R^{m-1}, which is always much less than 1. The loss in intensity for a particular ray can be minimized by properly selecting the mirror coefficients R and T. Assuming that the mirrors are perfect,

$$T + R = 1 \tag{13.36}$$

Substituting Eq. (13.36) into Eqs. (13.35) yields

$$I_m = K(R-1)^2R^{m-1} \sin^2 \frac{m\Delta}{2} \qquad m = 1, 2, 3, 4, \ldots \tag{a}$$

Differentiating this expression with respect to R yields

$$\frac{dI_m}{dR} = K \sin^2 \frac{m\Delta}{2} \{(R-1)[(R-1)(m-1)R^{m-2} + 2R^{m-1}]\} \tag{b}$$

Table 13.1 Optimum mirror properties for fringe multiplication

Multiplication factor m	R	T	Intensity coefficient T^2R^{m-1}
1	0	1	1
3	0.500	0.500	0.0625
5	0.667	0.333	0.0219
7	0.750	0.250	0.0111
9	0.800	0.200	0.0067

Setting Eq. (b) equal to zero and solving for R gives the reflection coefficient for the mirrors, which minimize the intensity lost as follows:

$$R = \frac{m-1}{m+1} \tag{13.37}$$

Since R is a function of m (the number of light traverses through the model), it is not possible to optimize the mirrors for all rays simultaneously. The optimum coefficients of reflection and transmission for each value of m are presented in Table 13.1. A multiplication factor of 5 is usually sufficient for most applications; hence, if only one set of mirrors is available, this set should be selected with $R = 0.667$ and $T = 0.333$ to optimize the minimum intensity condition.

EXERCISES

13.1 If a particular point in a photoelastic model is examined in a polariscope with a mercury light source ($\lambda = 548.1$ nm) and a fringe order of 3.00 is established, what fringe order would be observed if a sodium light source ($\lambda = 589.3$ nm) were used in place of the mercury source?

13.2 The stress fringe value f_σ for a material was determined to be 17.5 kN/m when sodium light ($\lambda = 589.3$ nm) was used in its determination. What would the stress fringe value for the same material be if mercury light ($\lambda = 548.1$ nm) were used in place of the sodium light?

13.3 Derive the equations for light passing through a stressed model in a plane polariscope with the polarizer and analyzer in parallel positions. Under what conditions does extinction ($I = 0$) occur?

13.4 Derive the equations for light passing through a stressed model in a plane polariscope (polarizer and analyzer crossed). Use an exponential representation for the light wave.

13.5 Derive the equations for light passing through a stressed model in a circular polariscope (arrangement C). Use a trigonometric representation for the light wave.

13.6 Derive the equations for light passing through a stressed model in a circular polariscope (arrangement D). Use an exponential representation for the light wave.

13.7 Determine the optical effects produced by light passing through a stressed model in a circular polariscope (arrangements A and B) with imperfect quarter-wave plates. Assume $\Delta = \pi/2 + \epsilon$ for the imperfect plates.

13.8 Determine the optical effects produced by light passing through a stressed model in a circular polariscope with imperfect quarter-wave plates. Use arrangements C and D for the polariscope and assume $\Delta = \pi/2 + \epsilon$ for the imperfect quarter-wave plates.